Biosis: Biological Systems (2021) 2(4), 423-439
https://doi.org/10.37819/biosis.001.04.0161

ORIGINAL RESEARCH

Exceptional Preservation of Feather Micro-Structures in Amber from the Middle-Cretaceous of Myanmar

Christian Laurent[1,2], Xia Wang[*,3], Bo Wang[4] & Zhiheng Li[*,5]

[1]*Aerodynamics and Flight Mechanics, University of Southampton, University Road, Southampton SO171BJ, United Kingdom, christian_laurent@live.com;*

[2]*Department of Geology, Babeș-Bolyai University, Str. Republicii (Gh. Bilașcu) nr.44, Cluj-Napoca, 400015, Romania;*

[3] *School of Biological Science and Technology, University of Jinan, 336 Nan Xinzhuang West Road, Jinan 250022, Shandong, China, bio_wangx@ujn.edu.cn.*

[4]*Nanjing Institute of Geology and Palaeontology, Chinese Academy of Sciences, Nanjing, China, bwang@nju.edu.cn*

[5]*Institute of Vertebrate Paleontology and Paleoanthropology, Chinese Academy of Sciences, 142 Xizhimenwai Dajie, Beijing 100044, China, lizhiheng@ivpp.ac.cn; *Corresponding authors*

ABSTRACT

Feathers are under-represented in the fossil record because soft tissues do not usually preserve well in sedimentary sequences. Fossil feathers are nevertheless extremely important in resolving pattern and process related to the origin of dinosaur flight. In recent years, several feathers have been discovered which have been mummified in amber; these feathers are preserved in three dimensions with remarkable sub-microscopic details and are especially important for our understanding of the early development of feathers. In this paper, we describe a diverse assemblage of mid-Cretaceous feathers contained within seven pieces of amber that have been recovered from northern Myanmar (Burma). These pieces include pennaceous primary feathers, contour feathers and other rachis-dominated feathers, and a plumulaceous (downy) feather. Subcomponents of these feathers, such as barbs, barbules, and nodes are immediately recognizable. One extraordinary piece contains the distal remains of the first four primary flight feathers and a small number of possible hooklets. These pieces are discussed in terms of evolutionary development and comments are made on flight ability where appropriate. The feathers are classified and compared with similar structures seen in Mesozoic and extant birds. We consider that integumentary feathers and feather-like structures fall within two major structural categories (shafted and non-shafted).

ARTICLE HISTORY

Received: 16-10-2021
Revised: 21-12-2021
Accepted: 28-12-2021

KEYWORDS

Feather
Microstructure
Amber
Cretaceous
Rachis
Flight

Introduction

The number of feathers described in the fossil record has increased dramatically since the 1990s (Alonso et al., 2000; Fountaine et al., 2005; Perrichot et al., 2008; Hu et al., 2009; Knight et al., 2011; Marugán-Lobón and Vullo, 2011; McKellar et al., 2011; Sayão et al., 2011; Thomas et al., 2014; de Souza Carvalho et al., 2015; Xing et al., 2016a, 2016b, 2017, 2018a, 2018b) and a

large proportion of the most recent descriptions have come from amber. Recent examples come from the United States (Grimaldi and Case, 1995), France (Perrichot et al., 2008) and, especially, Myanmar (Xing et al., 2016a, 2016b, 2017, 2018a; Peñalver et al., 2017). Mummified feathers allow a much greater insight and description than fossil feathers from sedimentary rocks because microstructure and even color can be preserved, and the fossils are usually presented in three dimensions. In contrast to these amber inclusions, when fossil feathers are preserved in sediments (*e.g.* those attached to fossil skeletons from the Jehol group of China), they normally form carbonized traces that do not preserve this level of detail (Kellner, 2002; Zhang et al., 2006; McKellar et al., 2011). Taphonomic processes also strongly favor lacustrine settings, and feathers preserved in amber are one of the most significant sources of fossil feathers from the terrestrial ecosystem (Davis and Briggs, 1995; Kellner, 2002). To that end, Burmese amber (Burmite) is perhaps the largest and most southerly source of well-preserved feathers from terrestrial dinosaurs, and it is hard enough to withstand the aggressive preparation and polishing necessary to make microstructural observations (Grimaldi et al., 2002; Nascimbene et al., 2014).

In spite of their rare preservation, the fossil record shows that modern-looking bird feathers were present and had diversified from earlier protofeathers by the mid-Cretaceous (Kellner, 2002; Xu, 2006; Zhang et al., 2006; Xu and Guo, 2009; Xu et al., 2010; Xing et al., 2016a), and the developmental hypothesis proposed by Prum (1999) and furthered by Xu (2006) for feather evolution is now widely (Ji et al., 2001; Wu et al., 2004; Benton, 2005; Heers and Dial, 2012; Heers et al., 2014; Li et al., 2017) but not completely (Sawyer and Knapp, 2003) accepted. As more fossil feathers are described, continued research should develop existing hypotheses for the evolution of these structures onto date-calibrated phylogenies, confirm microstructural positions with better preserved specimens, and further uncover the timeline of these evolutionary innovations.

Feathers preserved in amber become particularly useful when considering more derived characters, because mechanical performance was the principal selection pressure in the later stages of feather evolution, and many of the mechanically relevant features are both microscopic (Prum and Brush, 2002) and three-dimensional (Lees et al., 2017). The specimens in this work were all recovered from Burmite, which was deposited 98.8 ± 0.62 Mya (Late Albian-early Cenomanian) (Shi et al., 2012) but evidence of reworking and biostratigraphy suggests the amber might be older than its matrix and may be as old as 105 Ma (Cruickshank and Ko, 2003; Ross et al., 2010; Smith and Ross, 2018). However, there are major amber deposits around the globe, all of them have been deposited since the Cretaceous and all of them are likely to contain avialan remains (Grimaldi et al., 2002; Penney, 2010).

Materials and methods

Seven pieces of amber containing feather sections were collected from an amber mine located near Noije Bum Village, near the Tanai township (Myitkyina District, Kachin Province) in northern Myanmar (Figure 1). The amber in this region comes from a single species of coniferous tree from a forest with a tropical climate (Grimaldi et al., 2002; Cruickshank and Ko, 2003; Smith and Ross, 2018). The amber deposits in this region occur within lignitic seams that are between 30 cm and 40 cm thick and can be up to 12 m deep. All seven pieces are deposited in Nanjing Institute of Geology and Palaeontology, Chinese Academy of Sciences, Nanjing, China, where they have received collection numbers NIGP001 – NIGP007.

Specimens were prepared by removing as much

amber as possible with lapidary papers and finished with polishing compound. The intention was to polish within a few millimeters of the inclusion and in the same plane. In cases where this has proved possible this approach facilitates the use of large objective lenses, but such preparation is more difficult and sometimes not applicable for curved inclusions.

Prepared pieces were photographed using a millimeter-scale stand with a Zeiss Axio A2 polarizing light microscope (Oberkochen, Germany) under transmitted light. Inclusions are described following the terminology of Lucas and Stettenheim (1972), Proctor and Lynch (1993) and Sick et al. (1993) and are assigned where possible to stages from the hypothesis for feather evolutionary development (Prum and Brush, 2002). Specific proportions of these feathers, including rachis length, rachis diameter, and where possible the length, density, and angle of attachment of barbs and barbules, were measured from images using the FIJI (ImageJ) software package (Schindelin et al., 2012).

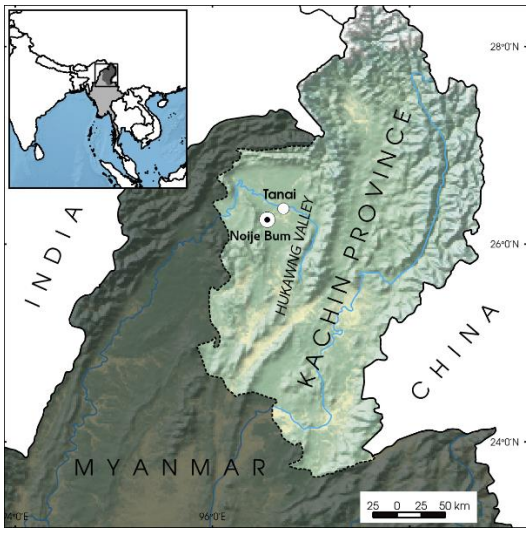

Figure 1. Material was recovered from the Noije Bum locality near the Tanai township, in the Hukawng Valley of Kachin Province, Myanmar.

Results

The specimens present three distinct forms. The first morphotype matches well with the modern contour feather. Contour feathers have a flattened arrangement of barbs and a long, broad rachis. Flight feathers are a type of contour feather. The second is the rachis-dominated feather (RDF), which may have been derived from a typical pennaceous feather (Wang et al., 2014; Xing et al., 2018b) and sometimes resemble modern rectrices. The RDF morphotype has elongate barbules, flexible barbs, and an absent, poorly-defined, or crescent shaped rachis. There is also a third morphotype which resembles a modern down feather, with a calamus but no rachis, and a fluffy appearance (Lucas and Stettenheim, 1972).

Detailed Description of Amber Pieces

NIGP001—measures approximately 42 mm × 27 mm × 9 mm and weighs 6.06 g (Figure 2),

This piece contains the distal parts of the four leading primary flight feathers, which have been preserved as if they were still articulated with the wing when the feathers were encapsulated. Unfortunately, the proximal parts of the feathers and the skeletal attachment is not preserved. The feathers are termed P1 to P4 where P1 denotes the leading primary. The feathers are deeper than the focal distance of the 20x objective from the surface and the focal plane of the 10x objective is too thin to observe the feathers in a meaningful way because they are out-of-plane; the feathers are observable with smaller objectives only. It was not possible to obtain some measurements of P3 and P4 because they overlap each other. All these feathers are brown in color and their rachises also appear to be melanized. The apices of the vane are pointed.

P1—This feather is smaller than P2 – P4. The preserved rachis measures 18mm. The vane is clearly asymmetrical, and the rachis is situated at 20% chord length from the leading edge. There is

no emargination. Total vane width is 6.1 mm. Leading barbs measure 4-4.5 mm and barb angle is 13°. Trailing barbs measure 6-6.5 mm and barb angle is 15° close to the rachis but changes to 40° for the last two thirds of the trailing vane's width. Barbs are paired and spaced 0.7 mm apart. Barbules are approximately 0.023 mm in length and spaced 80 μm apart. Barbule angle is 30°. A small number of hooklets are present, mostly at the distal termination of barbs though there are a very small number of some irregularly-spaced hooklets as well.

P2—The preserved rachis measures 29mm. The vane is clearly asymmetrical. The vane is 6.5-7 mm wide, and the rachis is situated between 10 and 15% chord length. There is no emargination. Barbs on the leading vane are approximately 4.5 mm long, and barb angle is 15°. Trailing barbs are approximately 8 mm long and the barb angle is 20° close to the rachis but increases to 35° halfway through along the trailing vane and returns to approximately 25 degrees at the edge of the vane. Barbs are paired and spaced 0.5 mm apart). Barbules have similar proportions to those of P1. Hooklets are also observed in the distal vane.

P3—The preserved rachis measures 27 mm. The vane is clearly asymmetrical. The vane is approximately 6.3 mm and the rachis is situated at 15% chord length. Leading barbs measure approximately 4.7 mm, and the barb angle is between 15 and 20°, trailing barbs are approximately 8 mm and the barb angle is 20°. Barbs are paired with 0.55 mm spacing. Barbules are not easily observable but appear to have similar proportions to the leading feather. Hooklets are not observable because of the way that this feather overlaps the next.

P4—The preserved rachis measures 24.5mm. The vane is clearly asymmetrical. The vane is approximately 6 mm and the rachis is situated

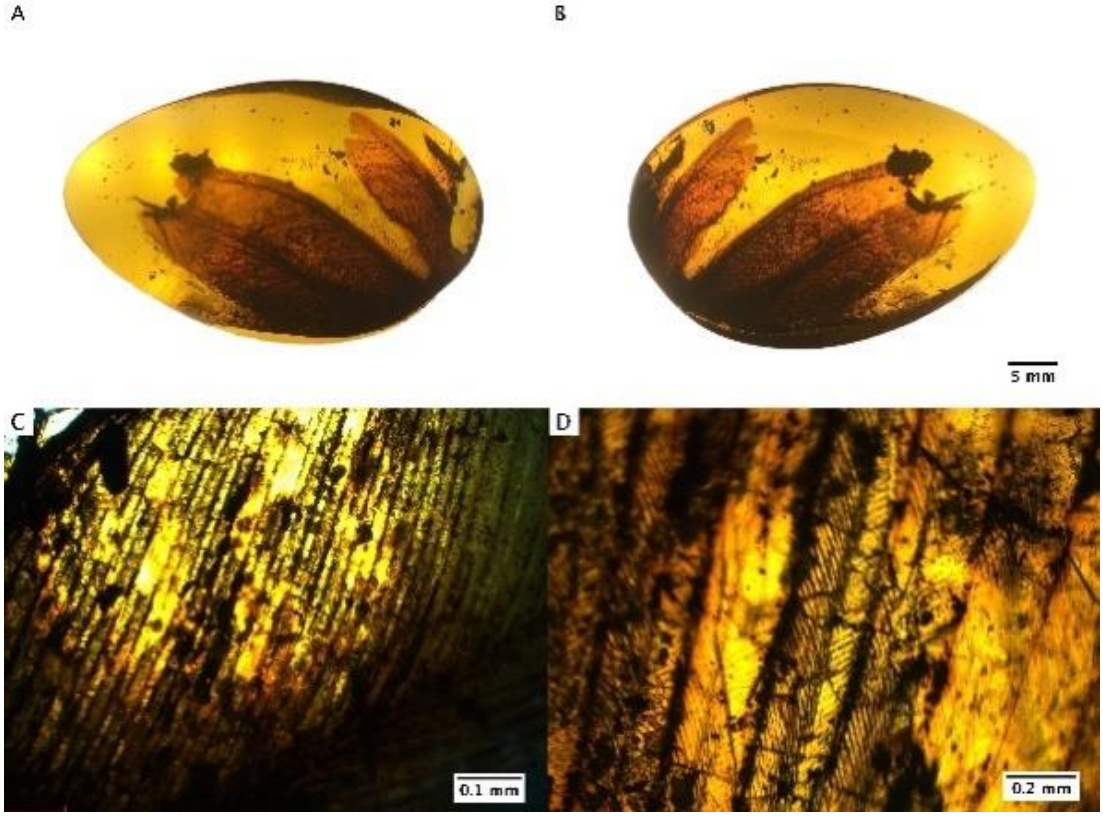

Figure 2: NIGP001 is an exceptional piece, which contains the distal remains of four primary flight feathers. Subfigures of increasing scale show the dorsal (A) and ventral (B) aspects of the whole piece, the trailing penna of the leading feather (C) and a close-up of overlapping barbules (D).

between 10 and 15% chord length. Leading barbs measure approximately 4.7 mm and the barb angle is between 15 and 20°, trailing barbs are approximately 8 mm, and the barb angle is 20°. Barbs are paired, with 0.55 mm spacing. Barbules measure between 20 and 30 μm, with 75 μm spacing. Barbule angle is approximately 40°. Hooklets are also observed in the distal vane.

Diagnosis—These feathers all have developed rachises, with two ordinal branches from the rachis that form a pennaceous vane and interlock distally. This would correspond to morphotype V from Prum and Brush (2002).

These feathers belonged to an animal which can be assigned to crown group Aves, since characteristics are almost identical to modern morphotypes.

NIGP002—measures approximately 26 mm × 12 mm × 3 mm, and weighs 0.57 g (Figure 3).

An almost-complete rachis-dominated feather. A rachis, barbs and barbules are clearly observable in this specimen and the shaft measures more than 15 mm. The rachis is almost completely preserved and only a small part of the calamus is missing. Distally, vane geometry suggests that approximately a third of the total shaft length was not preserved. The shaft is wide at the base and tapers from a proximal diameter of approximately 1 mm to approximately 0.3 mm distally. The shaft is slightly curved and suggests the feather was either on the left wing or left side of the tail. We consider it is more likely to be from the tail because of similarities to pieces described by Xing et al.(2018b) and because there have been a number of feathers described in pairs, which would be unlikely to preserve together if they were from the wings. The proximal rachis is vaneless. The vane starts around halfway along the preserved material. Average barb length is between 5 and 6 mm with average spacing 0.43 mm. There is no emargination. The barb angle on the leading vane (measured from the bending axis, not the tapering rachis edge) is 19° close to the rachis and 28° in the outer vane. The trailing vane is 21° close to the rachis, 42° mid-vane and 37° on the trailing edge, which indicates very clear asymmetry, as with modern birds. The vane width ratio is 2:3. Barbules are present all along the barbs. Average barbule length is 0.6 mm with 0.036 mm spacing.

The barbule angle of this specimen measures between 25° and 35° on the distal side of the barbs and between 45° and 55° on the proximal side. Nodes are visible along the barbules spaced at approximately 0.06 mm. These barbules overlap their proximal counterparts of the adjacent barb by approximately half their length and make for a semi-closed structure.

The calamus is pigmented with melanin. Rachis melanization is more variable and shows different preservation of carbonaceous traces and the distal half of the preserved rachis material, which would have been the middle of the whole shaft, is only slightly pigmented along its edge. There is a dark (pigmented) line along the length of the rachis which indicates the ventral groove. This pigmented line (and perhaps the groove as well) continues along the entire length of preserved rachis. There is no visible umbilicus. The vane presents a yellow coloration.

Diagnosis—An asymmetrical vane is the hallmark feature of Stage V development (Prum and Brush, 2002). Many characteristics are identical to modern pennaceous morphotypes, though the medial stripe and proportionally-wide rachis assigns this feather to the RDF morphotype. The feather probably comes from an enantiornithine (Xing et al., 2018a, 2019).

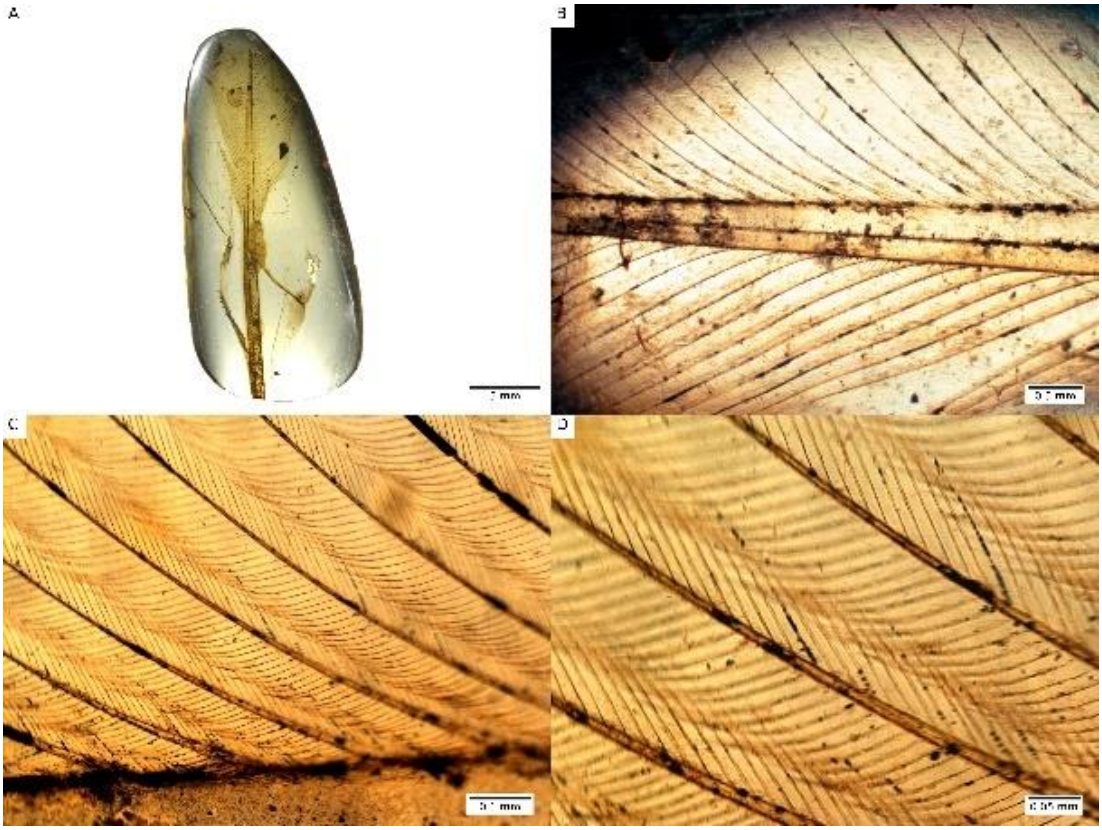

Figure 3: NIGP002 is an almost complete, open-vaned, asymmetrical flight feather. Subfigures o increasing scale show (A) the whole specimen, (B) the ventral aspect of the rachis and the ventral groove (C) the vane with overlapping barbules and (D) a close-up of melanization in the barbs.

NIGP003—measures approximately 20 mm × 12 mm × 3 mm and weighs 0.45 g (Figure 4).

This piece contains the distal 48 mm of a pennaceous feather. The rachis has a diameter of 1.45 mm at the most proximal location preserved and tapers to a point. The vane appears to be symmetrical based on barb measurements at the tip of the feather, but one side of the vane is only partially preserved so this cannot be confirmed. Barb angle is approximately 35°, barbules are present along the entire ramus. Barbs are spaced every 0.43mm. Barbule angle is 45° and barbules are spaced. Barbules are spaced 50 μm apart. Barbule nodes are not observed, hooklets are not observed and the vane is open. There is little pigmentation, but a ventral line does indicate a ventral groove. The distal shape of the vane looks to have degraded or been bitten.

Diagnosis—This feather is pennaceous. It has a bipinnate open vane and can be assigned to stage IV of evolutionary development (Prum and Brush, 2002). The medial stripe suggests the RDF morphotype however, so that placement in the evolutionary hypothesis is tentative.

NIGP004—This specimen measures approximately 28 mm × 13 mm × 3 mm, and weighs 0.7 g (Figure 5).

This specimen is an almost complete rachis dominated feather with nearly symmetric vanes. It is small and dart / wedge shaped. The preserved shaft measures 23.8 mm though a small piece of the proximal rachis is missing. The diameter of the shaft tapers from 500 μm at the base to a point at the very tip of the rachis. Barbs are pennaceous and barb length ranges between 230 μm proximally and 360 μm in the mid-vane.

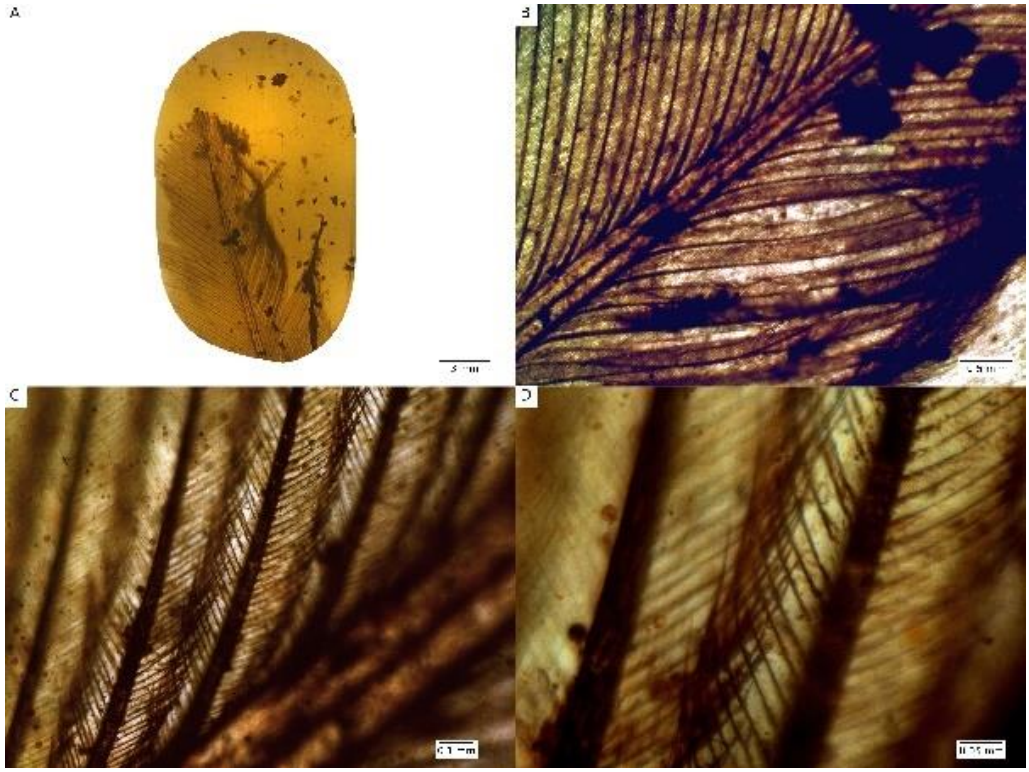

Figure 4: NIGP003 contains a partially complete pennaceous feather. Subfigures of increasing scale show (A) the whole piece, (B) the ventral aspect of a tapering rachis, (C) barbs with overlapping barbules and (D) an enlargement of paired barbules which do not have hooklets.

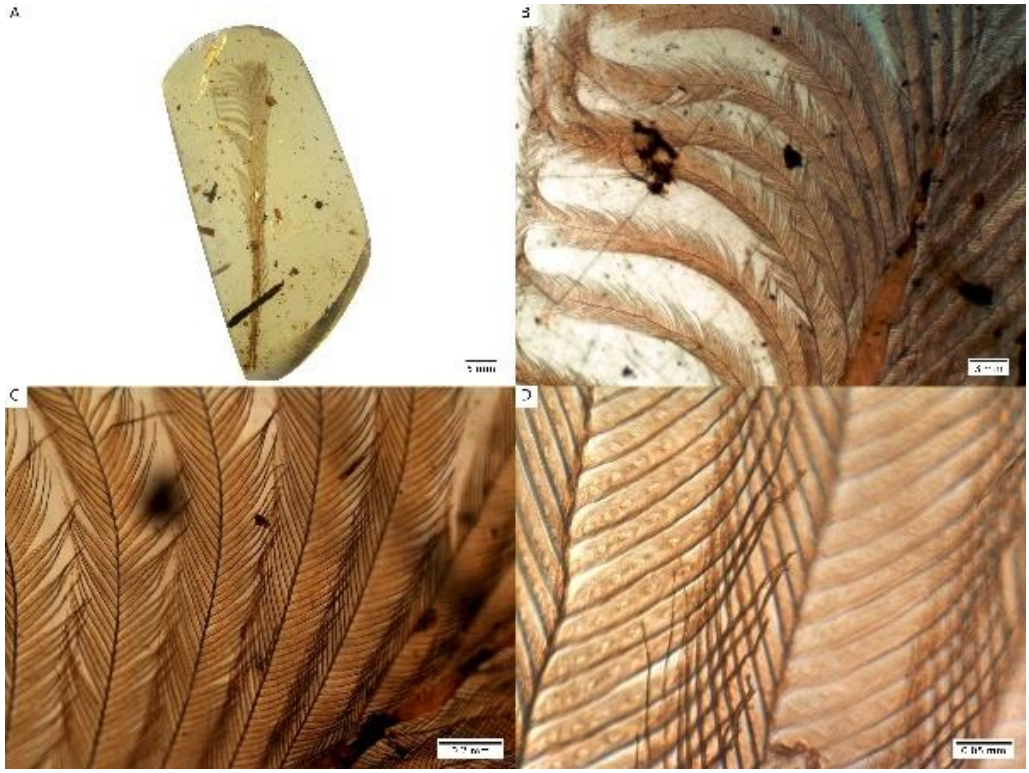

Figure 5: NIGP004 is a complete RDF. Subfigures of increasing scale show (A) the ventral aspect of the whole specimen in amber, (B) the distal penna with a buckled rachis, (C) a close-up of filamentous barbs and (D) a close-up of pennaceous, blade-like barbules. Color artifacts were removed using the GIMP software package.

Only one side of the vane has been preserved in its natural position and barb angle is approximately 27°. Blade-like barbules are present along the length of the barbs and hooklets are observed in the distal vane though not regularly present. Barbule angle is approximately 45° and barbules overlap with barbules from adjacent barbs. The rachis is proximally pigmented, and a pigmented line indicates the ventral groove. The vane presents a light brown coloration. Pennula are present in the distal vane but do not appear to be regularly distributed. Those pennula resemble those from previous work (McKellar et al., 2011; Xing et al., 2016a, 2017).

Diagnosis—An ornamental rachis-dominated feather. This specimen represents the morphotype IV of the Prum & Brush (2002) evolutionary model, because there is a long, broad rachis but no observable hooklets.

NIGP005—measures approximately 11.03 mm × 14.47 mm × 2.22 mm, and weighs 0.25 g (Figure 6).

This specimen is a complete contour feather. Ten barbs vary in length but average 1.8 mm. They are tufted and originate from a small calamus which is 0.6 mm in length. Reduced pennaceous barbules (Lucas and Stettenheim, 1972) are filamentous but thick, paired, and measure approximately 0.175 mm.

The calamus is a much darker color than the rest of the feather, which has a yellowy-brown, shiny color that suggests the presence of pyrites.

Diagnosis—NIGP005 resembles an extant contour feather and can be assigned to stage IIIa + b as barbs branch from a weakly developed rachis.

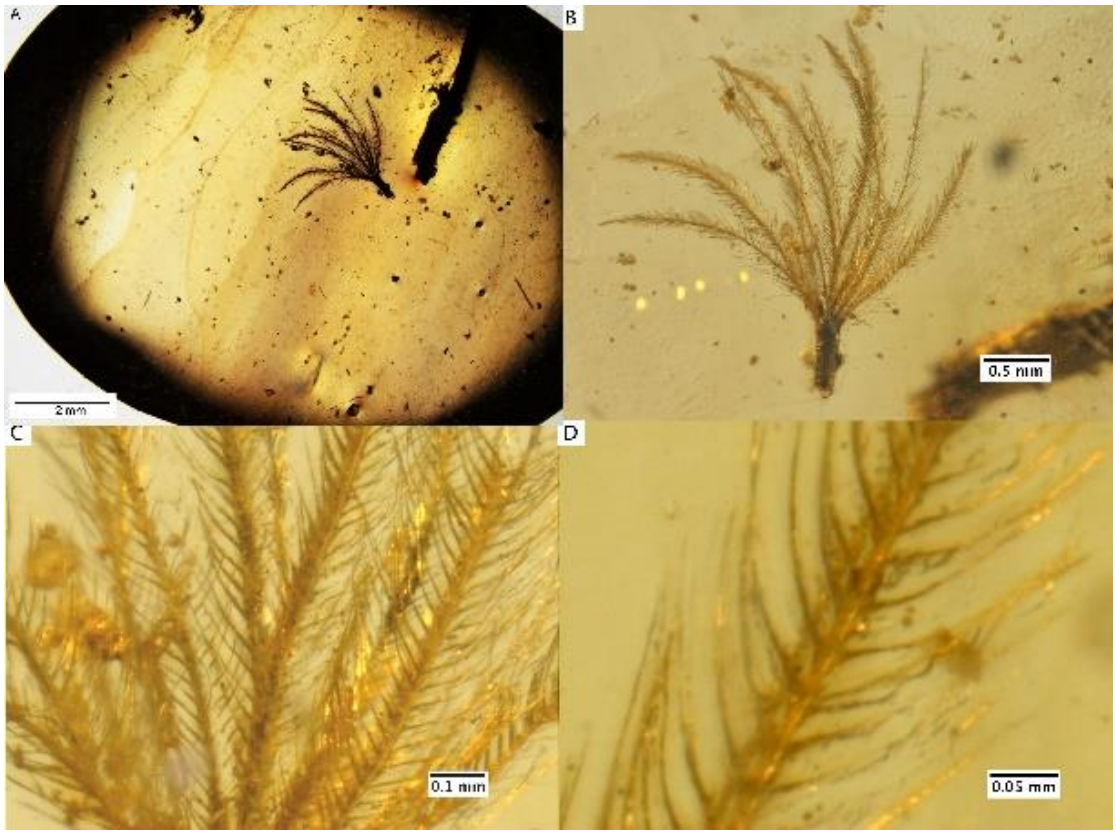

Figure 6: NIGP005 contains a downy-type feather. Subfigures of increasing scale show (A) the whole piece of amber, (B) the feather, (C) a branched barb, in which both branches have paired barbules and (D) a close-up of a single barb with thick, paired barbules.

NIGP006—measures approximately 19 mm × 19 mm × 5 mm, weighs 1.21 g (Figure 7).

This piece contains three un-shafted feathers, each approximately 0.5 mm in length and some individual pennaceous barbs. Two feathers are tufted at the basal part and may be covered by sheath and represent an immature state. Rachises are not developed, or they are very slim. Barbs are long and slender with flattened, paired barbules. Nodes are not observed and no hooklets are observed on any of these specimens. All barbs are pigmented and show brown coloration. They are plumulaceous, likely down feathers where barbs are open vaned.

Diagnosis— This specimen has plumulaceous feather morphology. Since these specimens have no developed rachis, and a fluffy aspect, dimension, and morphology, this feather is probably downy feather. Alternatively, it could be a contour feather that transitions from a pennaceous apex to a plumulaceous base (Lucas & Stettenheim, 1972; Sick, 1984; Proctor & Lynch, 1993) (stage IIIa + b).

NIGP007—measures approximately 15 mm × 13 mm × 4 mm, and weighs 0.43 g (Figure 8).

A downy feather with a barb which is longer than the rest and appears to be pennaceous. The calamus measures approximately 2 mm and the barbs measure approximately 3 mm, except for one very long barb, which appears to be pennaceous and measures approximately 5 mm. The barbules are filamentous, appear quite slender, and are not paired. There is no rachis. Barbules measure approximately 400 μm and their density were 16 over 0.2 mm (on both sides), or 80 mm^{-1} with variable spacing between 10 and 50 μm of the long barb.

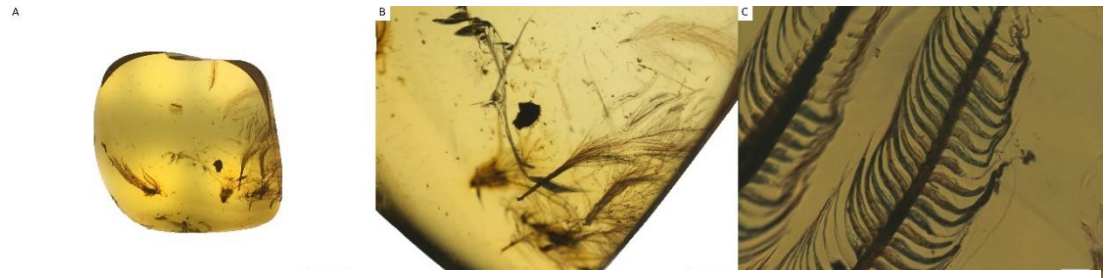

Figure 7: (A) NIGP006 contains (B) three downy feathers (C) with a close-up of a barb.

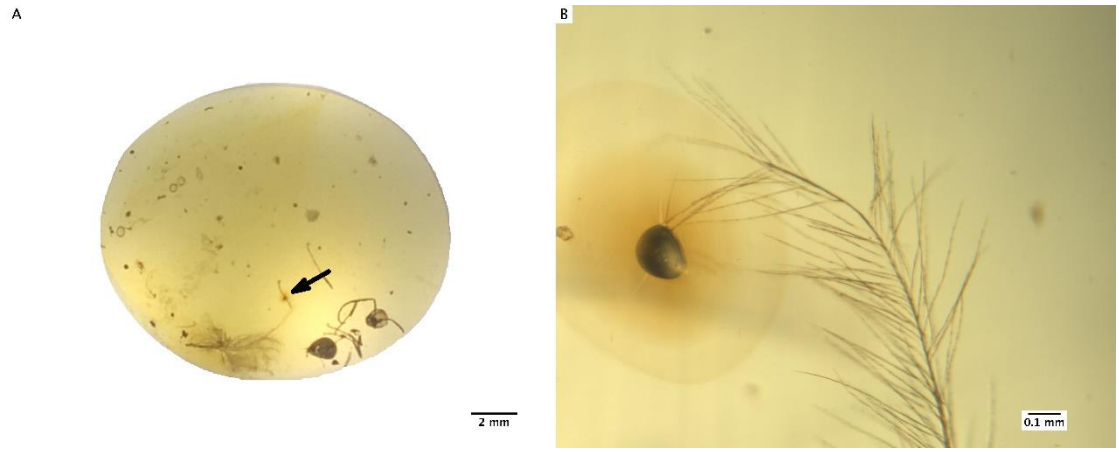

Figure 8: Piece number 7 (NIGP 007) contains an individual barb. The whole piece is shown in subfigure (A), Subfigure (B) shows the barb with a larger scale. The arrow in Subfigure A points to the detritus shown in Subfigure B.

Diagnosis—Likely a downy feather which can be assigned to stage IIIb from the evolutionary hypothesis. The long barb, and pennaceous barb morphology, is not easily explained.

Discussion

Five of the seven pieces described in this work are single feathers. Single feathers, especially small feathers, are more likely to be preserved than whole animals for taphonomic reasons. Feathers, insects, and small pirces of plant matter are preserved when resin, exuded as small blobs, engulfs them as it drips down the trunk of a tree (Ross, 1998). NIGP001, which contains four feathers, and the even more complete pieces recently described by Xing *et al.* (Xing et al., 2016a, 2016b, 2017, 2018a, 2018b, 2019, 2020a, 2020b; Carroll et al., 2019) would have formed in exceedingly rare circumstances as dripping amber formed a pool over material at the bottom of a tree, or from a massive flow down the side of a tree (Martínez-Delclòs et al., 2004).

Xing *et al.* have assigned two precocial wings and two incomplete partial hatchlings from the Burmese amber, to Enantiornithes. Their work tentatively indicates the dominant taxa in this area and niche, and suggests that the feathers described in this work, which are roughly the same size (like a modern Hummingbird), also came from enantiornithine individuals. The group is well-documented, successful, and diverse in the mid-Cretaceous. Studies which consider Mesozoic flight ability establish them as able fliers (Chiappe and Calvo, 1994; Norell et al., 2001; Chiappe and Walker, 2002; Rayner et al., 2002; Nudds et al., 2004; Wang et al., 2011; Liu et al., 2017; Serrano et al., 2018) and the pieces described in this work share many correlate features of flight ability, see Table 1.

Specimen	Summary	Stage of Development according to the Evolutionary Hypothesis	Vane Interlocking Mechanism (F, Friction / HG, Hook and Groove / SL, Slide lock)	Flighted individual? (L, Likely / N, not likely / U, unclear
NIGP001	4 primary flight feathers	V	F / HG	L
NIGP002	Proximal part of a rachis dominated feather	IV	F / HG	L
NIGP003	Distal part of rachis dominated feather	IV	F	U
NIGP004	A whole rachis dominated feather	IV	F / HG	L
NIGP005	A branched contour feather	IIIa + b	-	U
NIGP006	2 contour feathers	IIIa + b	-	U
NIGP007	A downy feather with a single long barb	IIIa + b	-	U

Table 1. Summary of specimen description. F = Friction; HG= Hook and Groove; SL = Slide lock; L= Likely; N= Not likely; U=unclear.

Flight Ability—Exactly when the modern capacity for powered flight evolved remains ambiguous, but Feo *et al.* (2015) concluded that it must have evolved crownward of *Confuciusornis* and long after the appearance of asymmetrical feathers. It seems that there might not be any single adaptation to flight (Feduccia and Tordoff, 1979; Norberg, 1985; Rayner, 1988; Clarke, 2013; Dyke et al., 2013; Feo et al., 2015; Lees et al., 2017) which diagnoses powered flight ability in the modern sense, but there are a number of adaptations which correlate with improved flight ability, and which are increasingly observed together in crownward groups.

Asymmetry in the flight feathers (a larger-scale, easily-observed adaptation) is a necessary (but not sufficient) adaptation to flight as the aerodynamic center of pressure is approximately under the one-third or one-quarter chord position (Feduccia and Tordoff, 1979; Norberg, 1985, 1995; Feduccia, 1999). In four of the pieces described above, this feature is clear, and the material resembles modern taxa.

In modern taxa, that the rachis is only 10-15% from the leading edge is thought to be an adaptation for aeroelastic tailoring, which means that a feather passively reduces the angle of attack (and therefore lift) when hit by a gust (Norberg, 1985). The evolutionary development of this adaptation has not been the subject of any detailed work.

The backward curvature of the rachis is another adaptation to flight seen in most modern birds, which seems to be another means to accomplish the automatic pitch-controlling effect (Norberg, 1985). This feature is strongly observed in all feathers from pieces NIGP001. The feathers in exhibit strongly curved, asymmetric feathers and might represent the most asymmetric feathers yet reported in a Mesozoic bird (Feo et al., 2015).

Barb shape and barbule overlap are less observable in most fossil feathers, and frequently this is also true for amber pieces if they are fuzzy or blurred by other particles.

Derived morphology has been seen in the pieces described above; primitive plumulaceous type feathers have round plumulaceous barbs and barbules whereas modern flight feathers have developed a rigid and flattened shape with dorsal and ventral ridges, and barbules have a ventral tooth as well as hooklets to facilitate attachment (Lucas and Stettenheim, 1972). This progression also suggests a change in the mechanism by which the vane remains closed, able to reattach, and resistant to damage (Zhang et al., 2018).

In earlier feathers, before the innovation of hooklets, a closed vane might have been facilitated by friction between overlapping barbules (Ennos et al., 1995; Feo et al., 2015). More derived feathers exhibit a ventral tooth on the barbule as well as hooklets in the distal vane, which function as a hook-and-groove model (Kovalev et al., 2013; Sullivan et al., 2017). This has already been observed in enantiornithine birds from Burmese amber (Xing et al., 2016a, 2016b), and would ensure a closed penna and good displacement of air, but much less so than the fully-interlocked structure seen in extant taxa.

A similar openness or looseness (and higher air transmissivity) can be observed in secondarily flightless taxa, confirming that a tightly-closed vane is an important adaptation for flight (Livezey, 2003; Feo et al., 2015; Zhang et al., 2018). Extant feathers make use of a slide-lock mechanism with multiple barbules on each hook barbule and dorsal spines on bow barbules (Zhang et al., 2018).

Blade-shaped barb rami are observed in pieces NIGP001, NIGP002, and NIGP004, but not in NIGP003. This feather might not be a flight feather. This shape is also documented in other enantiornithine feather preservations (Xing et al., 2018c, 2018a, 2019). Pennula with developed cilia or perhaps hooklets are seen in pieces NIGP001 and NIGP004 though they are irregular, sparse, and not regularly spaced. Whilst feather cohesion must still be principally controlled by friction, the hooklets would have functioned to some extent according to the hook and groove model (Kovalev et al., 2013; Sullivan et al., 2017). These pieces then fit neatly on an evolutionary progression that suggests vane interlocking was first accomplished by friction (Feo et al., 2015), then by a hook-and-groove system, and by the slide-lock model (Zhang et al., 2018) in derived and extant taxa.

The question of whether the RDF morphotype

evolved from a normal pennaceous feather, in which the rachis is hollow and filled with pith, or whether it has an independent evolutionary pathway has not yet been answered. This work places the RDF morphotype either before or beside the development of hook-and-groove barb cohesion. So currently, there is an inconsistency in observing features that are associated with flight in rachis-dominated feathers with incomplete rachises that would probably not have been stiff enough for flight.

If the feathers from pieces NIGP001-004 are enantiornithine, then well-documented osteological features such as a developed ossified sternum, long coracoid, and raised keel would imply that this group of paravians was capable of at least some form of sustained, powered flight. These features have been documented in other material recovered from the same region by Xing et al. (2017, 2018a).

The feathers seem to indicate at least some flight ability and this phylogenetic position fits with previous suggestions that modern flight ability had not evolved far stem-ward of this clade (Vazquez, 1992; Senter and Edu, 2006; Nudds and Dyke, 2010; Allen et al., 2013; Feo et al., 2015). However, a large wing with similar feathers, recovered in the same amber deposit was recently placed stem-ward of the enantiornithine lineage (Xing et al., 2020a).

Considering many adaptations to flight (*e.g*. asymmetrical flight feathers and modern-like barb geometry) we can suggest that the specimens described here likely belonged to flighted birds but also map these pieces onto the hypothesis for feather development (Prum and Brush, 2002).

Feather evolution and development—Most feathers preserved in amber so far discovered are similar to extant feathers (Feduccia and Tordoff, 1979; Norberg, 1995; Foth et al., 2014). The great diversity of paravian feathers present by the mid-Cretaceous means that these integuments adapted and diversified quite fast. The stepwise hypothesis for feather development (Prum, 1999; Prum and Brush, 2002; Xu, 2006; Xu and Guo, 2009) posits that a helical displacement of barb ridges within the collar of the feather follicle gave rise to the rachis. It is not clear how suddenly this might have happened and the transition remains particularly unclear before stage III of the hypothesis (1999), which might have been the most critical stage of feather evolution in birds and non-avian dinosaurs according to Xu (2006).

The RDF morphotype may need to be expanded to include a complete rachis or subdivided to better characterize rachis-dominated feathers which include features associated with flight. The feathers described here do not offer much advancement other than that this development must have happened before the Middle Cretaceous, and probably stem-ward of Enantiornithes. However, the hooklets seen in pieces NIGP001(Fig 2) and NIGP004 (Fig. 5) look to be very similar to the hooklets seen by Xing et al., (2016a).

Acknowledgements

CL was supported by NERC, UK (NE/L002531/1) and by UEFISCDI, Romania (PN-III-P4-ID-PCE-2016-0572) and is also grateful for a SPITFIRE DTP travel scholarship. XW is supported by Shandong Provincial Natural Science Foundation, China (ZR2017QD013). ZHL is supported by the National Natural Science Foundation of China (No. 41772013).

We thank Colin Palmer and Gareth Dyke for their helpful comments.

References

Allen, V., K. T. Bates, Z. Li, and J. R. Hutchinson. 2013. Linking the evolution of body shape and locomotor biomechanics in bird-line archosaurs. Nature.

Alonso, J., A. Arillo, E. Barrón, J. C. Corral, J. Grimalt, J. F. López, R. López, X. Martínez-Delclòs, V. Ortuño, E. Peñalver, and P. R. Trincão. 2000. A new fossil resin with biological inclusions in lower Cretaceous deposits from Álava (northern Spain, Basque-Cantabrian basin). Journal of Paleontology.

Benton, M. J. 2005. Vertebrate Palaeontology. Blackwell Science, 455 pp.

Carroll, N. R., L. M. Chiappe, and D. J. Bottjer. 2019. Mid-Cretaceous amber inclusions reveal morphogenesis of extinct rachis-dominated feathers. Scientific Reports 9:1–8.

Chiappe, L. M., and J. Calvo. 1994. Neuquenornis Volans, a new late cretaceous bird (enantiornithes: Avisauridae) from Patagonia, Argentina. Journal of Vertebrate Paleontology.

Chiappe, L. M., and C. A. Walker. 2002. Skeletal Morphology and Systematics of the Cretaceous Euenantiornithes (Ornithothoraces: Enantiornithes); pp. in Mesozoic birds: above the heads of dinosaurs.

Clarke, J. A. 2013. Feathers before flight. Science 340:690–692.

Cruickshank, R. D., and K. Ko. 2003. Geology of an amber locality in the Hukawng Valley, Northern Myanmar. Journal of Asian Earth Sciences 21:441–455.

Davis, P. G., and D. E. G. Briggs. 1995. Fossilization of feathers. Geology 23:783.

Dyke, G., R. de Kat, C. Palmer, J. Van Der Kindere, D. Naish, and B. Ganapathisubramani. 2013. Aerodynamic performance of the feathered dinosaur Microraptor and the evolution of feathered flight. Nature Communications 4.

Ennos, A. R., J. R. E. Hickson, and A. Roberts. 1995. Functional morphology of the vanes of the flight feathers of the pigeon Columba livia. The Journal of Experimental Biology.

Feduccia, A. 1999. The Origin and Evolution of Birds. Yale University Press, Newhaven, CT, 466 pp.

Feduccia, A., and H. B. Tordoff. 1979. Feathers of *Archaeopteryx*: asymmetric vanes indicate aerodynamic function. Science (New York, N.Y.) 203:1021–2.

Feo, T. J., D. J. Field, and R. O. Prum. 2015. Barb geometry of asymmetrical feathers reveals a transitional morphology in the evolution of avian flight. Proceedings of the Royal Society B: Biological Sciences. 282.

Foth, C., H. Tischlinger, and O. W. M. Rauhut. 2014. New specimen of *Archaeopteryx* provides insights into the evolution of pennaceous feathers. Nature 511.

Fountaine, T. M. R., M. J. Benton, G. Dyke, and R. L. Nudds. 2005. The quality of the fossil record of Mesozoic birds. Proceedings of the Royal Society B: Biological Sciences 272:289–294.

Grimaldi, D. A., and G. R. Case. 1995. A feather in amber from the Upper Cretaceous of New Jersey. American Museum Novitates 3126:1–6.

Grimaldi, D. A., M. S. Engel, and P. C. NASCIMBENE. 2002. Fossiliferous cretaceous amber from Myanmar (Burma): Its rediscovery, biotic diversity, and paleontological significance. American Museum Novitates 3361:1–71.

Heers, A. M., and K. P. Dial. 2012. From extant to extinct: locomotor ontogeny and the evolution of avian flight. Trends in Ecology & Evolution 27:296–305.

Heers, A. M., K. P. Dial, and B. W. Tobalske. 2014. From baby birds to feathered dinosaurs: incipient wings and the evolution of flight. Source: Paleobiology 40:459–476.

Hu, D., L. Hu, L. Zhang, and X. Xu. 2009. A pre-*Archaeopteryx* troodontid theropod from China with long feathers on the metatarsus. Nature 461:640–643.

Ji, Q., M. Norell, K. Gao, S. Ji, and D. Ren. 2001.

The distribution of integumentary structures in a feathered dinosaur. Nature 410:1084.

Kellner, A. 2002. A review of Avian Mesozoic fossil feathers; pp. 389–404 in L. M. Chiappe and L. M. Witmer (eds.), Mesozoic birds: above the heads of dinosaurs. University of California Press, Oakland, CA.

Knight, T. K., P. S. Bingham, R. D. Lewis, and C. E. Savrda. 2011. Feathers of the Ingersoll Shale, Eutaw Formation (Upper Cretaceous) of eastern Alabama: the largest collection of feathers from north american mesozoic rocks. PALAIOS 26:364–376.

Kovalev, A., A. E. Filippov, and S. N. Gorb. 2013. Unzipping bird feathers. Journal of The Royal Society Interface 11:20130988–20130988.

Lees, J., T. Garner, G. Cooper, and R. Nudds. 2017. Rachis morphology cannot accurately predict the mechanical performance of primary feathers in extant (and therefore fossil) feathered flyers. Royal Society Open Science 4.

Li, A., S. Figueroa, T.-X. Jiang, P. Wu, R. B. Widelitz, Q. Nie, and C.-M. Chuong. 2017. Diverse feather shape evolution enabled by coupling anisotropic signalling modules with self-organizing branching programme. Nature Communications 8:ncomms14139.

Liu, D., L. M. Chiappe, F. Serrano, M. Habib, Y. Zhang, and Q. Meng. 2017. Flight aerodynamics in enantiornithines: Information from a new Chinese Early Cretaceous bird. PLOS ONE 12:e0184637.

Livezey, B. C. 2003. Evolution of flightlessness in Rails (Gruiformes: Rallidae): Phylogenetic, ecomorphological, and ontogenetic perspectives. Ornithological Monographs.

Lucas, A. M., and P. R. Stettenheim. 1972. Avian Anatomy: Integument (Agricultural Handbook 362). United States Department of Agriculture, Michigan, pp.

Martínez-Delclòs, X., D. E. G. Briggs, and E. Peñalver. 2004. Taphonomy of insects in carbonates and amber. Palaeogeography, Palaeoclimatology, Palaeoecology 203:19–64.

Marugán-Lobón, J., and R. Vullo. 2011. Feather diversity in the Barremian (Early Cretaceous) of Las Hoyas, Spain. Comptes Rendus - Palevol 10:219–223.

McKellar, R. C., B. D. E. Chatterton, A. P. Wolfe, and P. J. Currie. 2011. A diverse assemblage of Late Cretaceous dinosaur and bird feathers from Canadian amber. Science 333:1619–22.

Nascimbene, P. C., C. J. Dove, D. A. Grimaldi, and A. Schmidt. 2014. Exceptional preservation of feather microstructures in amber from diverse faunas (Theropoda: Paraves) during the Lower and mid-Cretaceous. 9th European Palaeobotany-Palynology Conference 113–114.

Norberg, R. A. 1985. Function of vane assymetry and shaft curvature in bird flight feathers: Inferences on flight ability of *Archaeopteryx*; pp. 303–318 in M. Hecht, J. Ostrom, G. Violh, and P. Wellnhofer (eds.), The Beginnings of Birds. Freunde des Jura-Museums, Eichstatt.

Norberg, R. A. 1995. Feather assymetry in *Archaeopteryx*. Nature 374:221.

Norell, M., J. M. Clark, and L. M. Chiappe. 2001. An embryonic oviraptorid (Dinosauria: Theropoda) from the Upper Cretaceous of Mongolia. American Museum Novitates 1–20.

Nudds, R. L., and G. Dyke. 2010. Narrow primary feather rachises in Confuciusornis and Archaeopteryx suggest poor flight ability. Science 328:887–9.

Nudds, R. L., G. Dyke, and J. Rayner. 2004. Forelimb proportions and the evolutionary radiation of Neornithes. Proceedings of the Royal Society B: Biological Sciences.

Peñalver, E., A. Arillo, X. Delclòs, D. Peris, D. A. Grimaldi, S. R. Anderson, P. C. Nascimbene, and R. Pérez-de la Fuente. 2017. Ticks parasitised feathered dinosaurs as revealed by Cretaceous amber assemblages. Nature Communications 8:1924.

Penney, D. 2010. Biodiversity of fossils in amber from the major world deposits. 304.

Perrichot, V., L. L. Marion, D. Neraudeau, R. Vullo, and P. Tafforeau. 2008. The early evolution of feathers: fossil evidence from Cretaceous amber of France. Proceedings of the Royal Society B: Biological Sciences 275:1197–1202.

Proctor, N., and P. Lynch. 1994. Manual of Ornithology : Avian Structure and Function. Yale University Press, New Haven, 288–289 pp.

Prum, R. O. 1999. Development and evolutionary origin of feathers. The Journal of Experimental Zoology 285:291–306.

Prum, R. O., and A. H. Brush. 2002. The evolutionary origin and diversification of feathers. The Quarterly Review of Biology 77:261–95.

Rayner, J. 1988. The evolution of vertebrate flight. Biological Journal of the Linnean Society 34:269–287.

Rayner, J., G. Dyke, V. Bels, J. Gasc, and A. Casinos. 2002. Evolution and Origin of Diversity in the Modern Avian Wing. In Vertebrate Biomechanics and Evolution (V. Bels, J. Crasc, and A. Casinos (eds.)). Bios Scientific Publishers, London, 297–317 pp.

Ross, A. 1998. Amber: The Natural Time Capsule. The Natural History Museum, London, 73 pp.

Ross, A., C. Mellish, P. York, and B. Crighton. 2010. Burmese Amber; pp. 208–235 in D. Penney (ed.), Biodiversity of Fossils in Amber from the Major World Deposits. Siri Scientific Press, Manchester.

Sawyer, R. H., and L. W. Knapp. 2003. Avian skin development and the evolutionary origin of feathers. Journal of Experimental Zoology. Part B, Molecular and Developmental Evolution 298:57–72.

Sayão, J. M., A. A. F. Saraiva, and A. M. K. Uejima. 2011. New evidence of feathers in the Crato Formation supporting a reappraisal on the presence of Aves. Anais Da Academia Brasileira de Ciencias 83:197–201.

Schindelin, J., I. Arganda-Carreras, E. Frise, V. Kaynig, M. Longair, T. Pietzsch, S. Preibisch, C. Rueden, S. Saalfeld, B. Schmid, J.-Y. Tinevez, D. J. White, V. Hartenstein, K. Eliceiri, P. Tomancak, and A. Cardona. 2012. Fiji: an open-source platform for biological-image analysis. Nature Methods 9:676–82.

Senter, P., and P. S. Edu. 2006. Scapular orientation in theropods and basal birds, and the origin of flapping flight. Acta Palaeontologica Polonica 51:305–313.

Serrano, F., L. M. Chiappe, P. Palmqvist, B. Figueirido, J. Marugán-Lobón, and J. L. Sanz. 2018. Flight reconstruction of two European enantiornithines (Aves, Pygostylia) and the achievement of bounding flight in Early Cretaceous birds. Palaeontology 61:359–368.

Shi, G., D. A. Grimaldi, G. E. Harlow, J. Wang, J. Wang, M. Yang, W. Lei, Q. Li, and X. Li. 2012. Age constraint on Burmese amber based on U-Pb dating of zircons. Cretaceous Research 37:155–163.

Sick, H. 1993. Birds in Brazil: A Natural History. Princeton University Press, 570 pp.

Smith, R. D. A., and A. Ross. 2018. Amberground pholadid bivalve borings and inclusions in Burmese amber: implications for proximity of resin-producing forests to brackish waters, and the age of the amber. Earth and Environmental Science Transactions of the Royal Society of Edinburgh 107:239–247.

de Souza Carvalho, I., F. E. Novas, F. L. Agnolin,

M. P. Isasi, F. I. Freitas, and J. A. Andrade. 2015. A Mesozoic bird from Gondwana preserving feathers. Nature Communications 6:7141.

Sullivan, T. N., M. Chon, R. Ramachandramoorthy, M. R. Roenbeck, T. T. Hung, H. D. Espinosa, and M. A. Meyers. 2017. Reversible attachment with tailored permeability: The feather vane and bioinspired designs. Advanced Functional Materials 27:1702954.

Thomas, D. B., P. C. Nascimbene, C. J. Dove, D. A. Grimaldi, and H. F. James. 2014. Seeking carotenoid pigments in amber-preserved fossil feathers. Scientific Reports 4:1–71.

Vazquez, R. J. 1992. Functional osteology of the avian wrist and the evolution of flapping flight. Journal of Morphology.

Wang, X., A. J. McGowan, and G. Dyke. 2011. Avian Wing Proportions and Flight Styles: First Step towards Predicting the Flight Modes of Mesozoic Birds. PLoS ONE 6:e28672.

Wang, X., J. K. O'Connor, X. Zheng, M. Wang, H. Hu, and Z. Zhou. 2014. Insights into the evolution of rachis dominated tail feathers from a new basal enantiornithine (Aves: Ornithothoraces). Biological Journal of the Linnean Society 113:805–819.

Wu, P., L. Hou, M. Plikus, M. Hughes, J. Scehnet, S. Suksaweang, R. B. Widelitz, T.-X. Jiang, and C.-M. Chuong. 2004. Evo-Devo of amniote integuments and appendages. The International Journal of Developmental Biology 48:249–70.

Xing, L., J. K. O'Connor, R. C. McKellar, L. M. Chiappe, M. Bai, K. Tseng, J. Zhang, H. Yang, J. Fang, and G. Li. 2018a. A flattened enantiornithine in mid-Cretaceous Burmese amber: morphology and preservation. Science Bulletin 63:235–243.

Xing, L., R. C. Mckellar, M. Wang, M. Bai, J. K. O 'connor, M. J. Benton, J. Zhang, Y. Wang, K. Tseng, M. G. Lockley, G. Li, W. Zhang, and X. Xu. 2016a. Mummified precocial bird wings in mid-Cretaceous Burmese amber. Nature Communications 7.

Xing, L., R. C. McKellar, X. Xu, G. Li, M. Bai, W. S. Persons, T. Miyashita, M. J. Benton, J. Zhang, A. P. Wolfe, Q. Yi, K. Tseng, H. Ran, and P. J. Currie. 2016b. A Feathered Dinosaur Tail with Primitive Plumage Trapped in Mid-Cretaceous Amber. Current Biology 26:3352–3360.

Xing, L., R. C. McKellar, and J. K. O'Connor. 2020a. An unusually large bird wing in mid-Cretaceous Burmese amber. Cretaceous Research 110:104412.

Xing, L., P. Cockx, and R. C. McKellar. 2020b. Disassociated feathers in Burmese amber shed new light on mid-Cretaceous dinosaurs and avifauna. Gondwana Research 82:241–253.

Xing, L., P. Cockx, R. C. McKellar, and J. K. O'Connor. 2018b. Ornamental feathers in Cretaceous Burmese amber: resolving the enigma of rachis-dominated feather structure. Journal of Palaeogeography 7:13.

Xing, L., P. Cockx, R. C. McKellar, and J. O'Connor. 2018c. Ornamental feathers in Cretaceous Burmese amber: resolving the enigma of rachis-dominated feather structure. Journal of Palaeogeography 7:1–18.

Xing, L., R. C. McKellar, J. K. O'Connor, M. Bai, K. Tseng, and L. M. Chiappe. 2019. A fully feathered enantiornithine foot and wing fragment preserved in mid-Cretaceous Burmese amber. Scientific Reports 9.

Xing, L., J. K. O'Connor, R. C. McKellar, L. M. Chiappe, K. Tseng, G. Li, and M. Bai. 2017. A mid-Cretaceous enantiornithine (Aves) hatchling preserved in Burmese amber with unusual plumage. Gondwana Research 49:264–277.

Xu, X. 2006. Feathered dinosaurs from China and the evolution of major avian characters.

Integrative Zoology 1:4–11.

Xu, X., and Y. Guo. 2009. The origin and early evolution of feathers: Insights from Recent paleontological and neontological data. Vertebrata Palasiatica 47:311–329.

Xu, X., X. Zheng, and H. You. 2010. Exceptional dinosaur fossils show ontogenetic development of early feathers. Nature 464:1338–41.

Zhang, F., Z. Zhou, and G. Dyke. 2006. Feathers and "feather-like" integumentary structures in Liaoning birds and dinosaurs. Geological Journal 41:395–404.

Zhang, F., L. Jiang, and S. Wang. 2018. Repairable cascaded slide-lock system endows bird feathers with tear-resistance and superdurability. Proceedings of the National Academy of Sciences of the United States of America 115:201808293.